Nanosecond Dynamics of Tryptophans in Different Conformational States of Apomyoglobin Proteins

ARTICLE *in* BIOCHEMISTRY · MARCH 2000

Impact Factor: 3.02 · DOI: 10.1021/bi992117+ · Source: PubMed

3 AUTHORS, INCLUDING:

Jay R Knutson
National Institutes of Health
106 PUBLICATIONS **3,108** CITATIONS

SEE PROFILE

Nanosecond Dynamics of Tryptophans in Different Conformational States of Apomyoglobin Proteins

Olga Tcherkasskaya,*,‡ Oleg B. Ptitsyn,‡ and Jay R. Knutson§

Laboratory of Experimental and Computational Biology, National Cancer Institute, National Institutes of Health, Bethesda, Maryland 20892, and Laboratory of Cell Biology, National Heart, Lung, and Blood Institute, National Institutes of Health, Bethesda, Maryland 20892

Received September 9, 1999; Revised Manuscript Received December 2, 1999

ABSTRACT: Fluorescence anisotropy kinetics were employed to quantify the nanosecond mobility of tryptophan residues in different conformational states (native, molten globule, unfolded) of apomyoglobins. Of particular interest is the similarity between the fluorescence anisotropy decays of tryptophans in the native and molten globule states. We find that, in these compact states, tryptophan residues rotate rapidly within a cone of semiangle 22−25° and a correlation time of 0.5 ns, in addition to rotating together with the whole protein with a correlation time of 7−11 ns. The similar nanosecond dynamics of tryptophan residues in both states suggests that the conformation changes that distinguish the molten globule and native states of apomyoglobins originate from either subtle, slow rearrangements or fast changes distant from these tryptophans.

Protein dynamics are of fundamental interest in efforts to reveal the molecular mechanisms of biological activity, both in defining the biological relevance of a "structure−function" relationship and in understanding protein recognition. Regarding protein folding, clearly, when protein folds from a nascent polypeptide chain, the dynamics of backbone and side chains inevitably influences both the kinetics of the process and the character of the final state achieved. However, despite current research interest in protein dynamics and the large number of studies ongoing, there are surprisingly few definitive data (rates and amplitudes) for peptide dynamics in different conformational states. Specifically, dynamic measurements are needed in studies of the "molten globule" state, which is thought to be a general intermediate in protein folding (*1*). A key assumption of this hypothesis, namely, increased mobility of side chains in the molten globule state, remains conjecture, in part, because the peptide backbone and side-chain dynamics are hard to separate and quantify. At present, no single technique is capable of yielding unequivocal results for both motions. In fact, only a few methods provide direct information about protein dynamics. Among these is fluorescence anisotropy, and it is particularly suited for investigation of macromolecules in dilute solution (*2*, *3*). The direct connection between anisotropy and internal mobility of fluorescent groups and the great sensitivity of macromolecular dynamics to intra- and intermolecular interactions (*2*) ensure the high potential of this technique in studies of protein folding. In general, fluorescence anisotropy methods do not require knowledge of the protein concentration. They are capable of using miniscule concentrations and thereby avoid aggregation. Successful application of anisotropy techniques to study macromolecules, however, is impossible without cognizance of the relaxation processes for residues used as reporters. In addition, a critical evaluation of the limitations of anisotropy data is necessary. For example, the accuracy of anisotropy data depends on the relative time scale of rotation and the fluorescence lifetime of the reporter. In steady-state fluorescence experiments, with variation of both protein dynamics (by addition of a viscous cosolvent) and fluorescence lifetime of the reporter (by addition of a quencher), the uncertainty in data may significantly increase through a series of samples. In proteins, one potential concern is about exposed and buried reporters in the molecular matrix. If the cosolvent (or quencher) affects only exposed reporters, then the relaxation times recovered by conventional steady-state methods may be distorted (*4*). In addition, the protein structure itself may be altered by the addition of cosolvent (*5*). Time-resolved anisotropy experiments are free of these shortcomings. Substantial information about protein dynamics can be obtained in a single experiment in the solvent of interest. The anisotropy signal is, however, a fluorescence intensity-weighted average; hence, it may be complex due to associative decay (*6*), i.e., a linkage of dynamic and fluorescence heterogeneity. The resulting heterogeneity may be resolved in some cases (*6*), but discrimination among reporters contributing to the total fluorescence spectrum presents difficulties. All of the potential problems noted above may underlie the diversity of results obtained for similar proteins by different fluorescence techniques. For example, relaxation times reported for overall rotation of native apomyoglobins cover a 2.5-fold range (*7*−*10*). Further, both increases and decreases of tryptophan mobility have been reported for the "molten globule−native" transition of apomyoglobin (*7*, *8*). Clearly, a better understanding of the factors that determine the fluorescence anisotropy of the

* To whom correspondence should be addressed. Telephone: (301) 496-9065. Fax: (301) 402-4724. E-mail: tcherkasskaya@nih.gov.

‡ National Cancer Institute.

§ National Heart, Lung, and Blood Institute.

10.1021/bi992117+ CCC: $19.00
Published on Web 01/22/2000

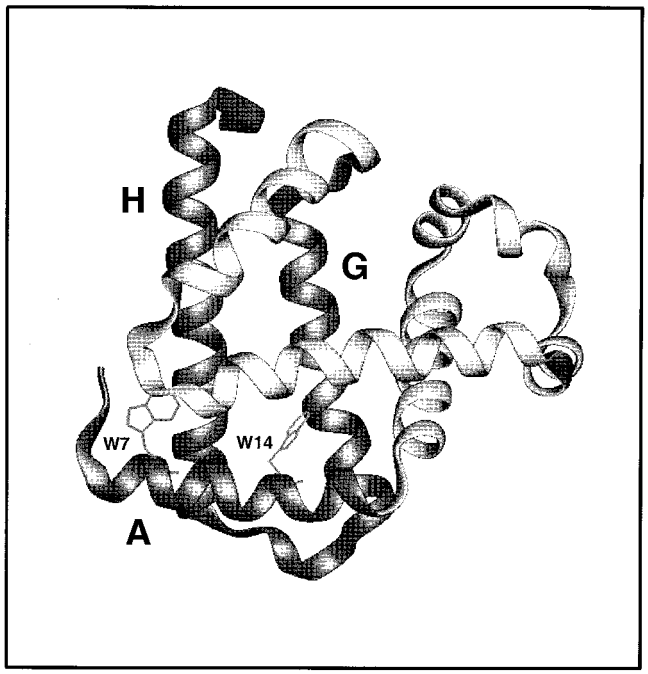

FIGURE 1: Ribbon representation of native apomyoglobin with tryprophan residues W7 and W14 residing to the A-helix. The native A-, G-, and H-helices become relatively stable at an early stage of protein folding and are relatively stable in the equilibrium molten globule state.

reporter and its relationship to protein structure is required to take full advantage of this information. This paper deals with this problem for tryptophan (Trp)[1] residues in apomyoglobins.

Apomyoglobin (apoMb) has been employed as a protein folding model system for over 30 years; thus, it is a good candidate for a kinetic study. First, the experimental conditions needed to reach a particular conformational state (native, molten globule, unfolded) are well-established by numerous experimental methods (*11*). Second, native apoMb is an α-helical protein with Trp residues known to reside on the A-helix (Figure 1). Third, efforts have previously been made to separate the fluorescence behavior of Trp residues by benign modification (*12*, *13*). The same goal can be achieved, however, by using either mutant proteins or various wild-type proteins with naturally occurring Trp replacements. We have studied sperm whale and horse globins with two Trp residues located at positions 7 and 14, along with tuna myoglobin possessing only a single Trp residue at position 14. The engineered proteins were sperm whale mutants with only Trp7 or only Trp14 (the other Trp residue was replaced by phenylalanine). The comparison of the data obtained for one-Trp globins (tuna and sperm whale mutants) with those of other species containing two Trp residues (sperm whale and horse) should highlight the effect of fluorescence heterogeneity on the composite anisotropy kinetics. In terms of protein structure, we focused on the nanosecond dynamics of Trp residues to explore the changes in intraprotein interactions involved in the "native−molten globule" transition.

[1] Abbreviations: apoMb, apomyoglobin; SDS, sodium dodecyl sulfate; Trp, tryptophan.

MATERIALS AND METHODS

Myoglobins. Horse myoglobin was purchased from Sigma. Sperm whale and tuna myoglobins as well as the sperm whale mutants containing one Trp residue with the other one replaced by the phenylalanine (W14F and W7F) were gifts of Dr. Oleg B. Ptitsyn (Institute of Protein Research, Puschino).

Apomyoglobins. The heme was removed by the 2-butanone method of Teale (*14*) followed by gel chromatography on Pharmacia columns PD-10 containing Sephadex G-25. The apoproteins were extensively dialyzed against water at 4 °C, and then lyophilized for storage. Contamination of the apoprotein by myoglobin was assessed spectrophotometrically; no significant absorption was observed in the Soret region for either one- or two-Trp apoproteins. The homogeneity of the apomyoglobin was tested by SDS-polyacrylamide gel electrophoresis (*15*). A single band was always observed for samples investigated. The protein concentration was estimated by absorbance at 280 nm with a Hewlett-Packard 8452A diode array spectrophotometer. The molar extinction at 280 nm was calculated from the tryptophan and tyrosine composition and the standard values of 5690 and 1280 [$M^{-1}\cdot cm^{-1}$] reported for those amino acids (*16*).

Chemicals and Solutions. The experiments were done at room temperature in a 10 mM sodium acetate, 10 mM sodium phosphate buffer mixture, containing 30 mM NaCl. To reach the native and molten globule states, the pH of the protein solutions were adjusted to 6.5 and 4.2, respectively (*11*). The unfolded state was reached by addition of 8 M urea to the native solution. All reagents were of reagent grade or better. Ultrapure urea was purchased from ICN (Irvine, CA) and used without further purification.

Steady-state Fluorescence Measurements. Fluorescence emission and excitation spectra were obtained on a SPEX Fluorolog-2 spectrofluorometer (data interval of 0.5 nm, scan speed of 50 nm/min) supplied with DM-3000 software. Emission was measured in the ratio mode and background fluorescence from a solvent blank was subtracted. Spectra were corrected for the wavelength-dependence of the instrument response.

Time-resolved Fluorescence Measurements. Time-resolved fluorescence measurement were done by the time-correlated single-photon counting technique essentially as described in (*17*). Samples were excited at 295 nm using a synchronously pumped, cavity-dumped, frequency-doubled dye laser (repetition rate of 4 MHz, pulse width of 5 ps, average UV power of <200 μW). The channel width was 85 ps, and the data were collected in 512 channels. Basically, the instrument is unable to resolve events faster than the temporal spread of photoelectrons inside the photomultiplier. The response of the system to a scattered laser pulse is referred to as the "lamp" or "impulse response function", and this is used for convolution. In present experiments, the instrumental time resolution was limited primarily by the detector (R955 photomultiplier, transit time spread of 900 ps). This allowed one to resolve the correlation times as short as 150 ps. Some samples were remeasured with a microchannel plate photomultiplier, with resolution approaching 50 ps (total optical and electronic transit time spread of 120 ps). This improvement, however, led to no changes in the recovered parameters.

Fluorescence intensity decay surfaces were collected under "magic angle" conditions for equal dwell times and by stepping the emission monochromator in increments of 5 nm in the range of 300−450 nm. More than 30 decays were obtained for each sample and simultaneously analyzed according to the global procedure (*18*), assuming that fluorescence intensity decay follows a multiexponential law,

$$I(t, \lambda) = \sum_{i}^{n} \alpha_i(\lambda) e^{-t/\tau_i} \quad (1)$$

The relative amplitudes, α_i, and the decay constants, τ_i, were the numerical parameters recovered. To resolve the emission spectra associated with the individual decay constant (decay-associated spectra, DAS), the fluorescence intensities at the various wavelengths were expressed as $\alpha\tau$ products, and the relative contribution of each decay component to the total fluorescence was calculated as $\alpha_i\tau_i/\Sigma\alpha_i\tau_i$ (*19*). In all cases, two decay times and third, short-lived, fixed component (compensating for any scattered excitation or color shift) gave the best fit.

To generate the anisotropy decay, $r(t)$, the fluorescence at 350 nm was monitored through a film polarizer oriented parallel, $I_{VV}(t)$, or perpendicular, $I_{VH}(t)$, to the vertical excitation polarization and alternatively recorded. Data were collected up to 20 000 counts in the peak. For each sample, 16 fluorescence intensity decays were obtained contemporaneously and summed to calculate the anisotropy decay, $r(t)$, as follows:

$$r(t) = \frac{I_{VV}(t) - GI_{VH}(t)}{I_{VV}(t) + 2GI_{VH}(t)} = \frac{D(t)}{S(t)} \quad (2)$$

where $D(t)$ and $S(t)$ represent the difference and sum functions, respectively. The factor G was reduced to unity with a wedge depolarizer (Optics for Research, DPU) placed 1 cm from the entrance slit of the monochromator. The parameters of the anisotropy decay were recovered from the experimental decays $I_{VV}(t)$ and $I_{VH}(t)$ by the "sum and difference" method assuming the nonassociative model (*20*). The reference lamp profile and color shift used for convolution analysis was tested with a monoexponential standard (melatonin aqueous solution with fluorescence lifetime τ_{fl} = 5.27 ns). The convolution was compared with the experimental decay by a nonlinear least-squares analysis. The best fit between the theoretical curve and the data was evaluated from the plot of weighted residuals, the autocorrelation function of the weighted residuals, and the reduced χ^2 value.

Evaluation of Intramolecular Mobility. The anisotropy decay $r(t)$ was considered to be a sum of discrete exponential functions:

$$r(t) = \sum_{i}^{n} \beta_i e^{-t/\phi_i} \quad (3)$$

where β_i and ϕ_i were the numerical parameters to be recovered. The analysis showed that two correlation times were needed to account for the fluorescence anisotropy decay data, as judged by χ_R^2 values of the fit. Attempted fits of the experimental data to a one- or three-exponential models showed a substantial increase in χ_R^2 value. A typical example of the analysis of the experimental data is shown in Figure 2, together with the statistical parameters used to judge the quality of the fit. Estimation of error in the fitting parameters was done using the "χ^2 − surface" plane method (*21*). An initial value of one of the variables was chosen and fixed, allowing the optimization routine to derive the others. By monitoring the χ^2 dependence for each value, one obtains the optimum set of parameters corresponding to the global χ^2 minimum (*22*). The uncertainty in the recovered variable was calculated on the basis of a 90% confidence interval (*21*), which usually corresponds to a 10% increase in the reduced χ^2 above the minimum value.

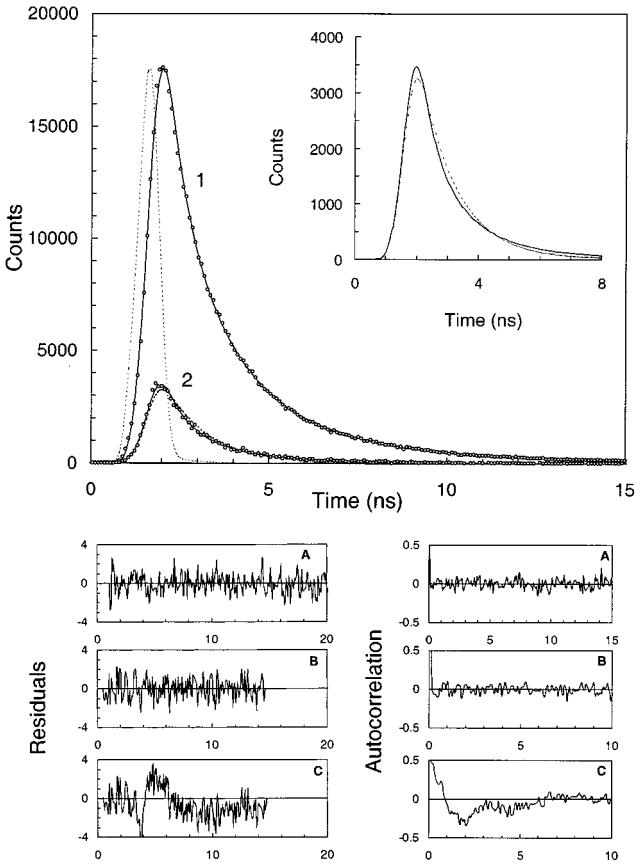

FIGURE 2: Analysis of the anisotropy kinetics by the sum and difference method (eq 2) for native apomyoglobin (sperm whale). The experimental data (circles), fitted curves (solid, dashed), and lamp profile (dotted) are shown. The best-fit parameters for sum curve (1) were $\alpha_1 = 0.64$, $\tau_1 = 1.33$ ns, $\alpha_2 = 0.36$, $\tau_2 = 4.12$ ns, and $\chi^2 = 1.20$ (solid, A). The best fit parameters for difference curve (2) were $\beta_1 = 0.05$, $\phi_1 = 0.52$ ns, $\beta_2 = 0.19$, $\phi_2 = 7.03$ ns, $\chi^2 = 1.36$ (solid, B). One exponential fit to the difference curve yielded $\beta = 0.35$, $\phi = 3.07$ ns, $\chi^2 = 2.68$ (dash, C). The inset shows the fitted difference curves. The weighted residuals and the autocorrelation function of the weighted residuals illustrate the quality of the fit. The excitation was set at 295 nm and emission was collected at 350 nm. The conditions were as described in Materials and Methods.

Tryptophan mobility was interpreted in the framework of a "two-time approximation" commonly used for macromolecular dynamics analysis (*2*, *23*). According to this model, the decrease of anisotropy is caused by a sum of "fast" and "slow" motions of the reporter. Time-resolved anisotropy experiments provide information on both, the amplitude of motion, β_i, and the time scale, ϕ_i, on which this motion occurs. In subsequent discussions, the relaxation time τ =

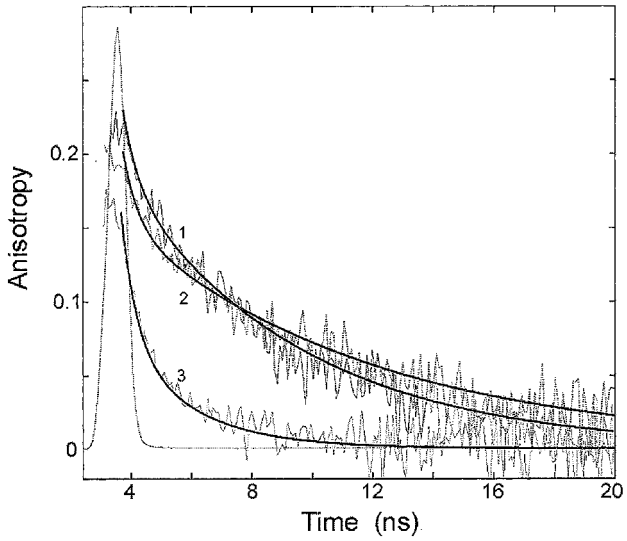

FIGURE 3: Time-resolved fluorescence anisotropy decay of sperm whale apomyoglobin in native (1), molten globule (2), and unfolded (3) states. Both the experimental data (noisy curves) and fitted data (smooth curves) are shown. A scaled lamp profile (dotted) is given for reference. The excitation was set at 295 nm, and emission was collected at 350 nm. The conditions were as described in Materials and Methods.

3ϕ will be used to compare the present data with prior results obtained by a conventional steady-state method. For the simplest case of rotational Brownian motion of a spherical particle or a rigid dumbbell in a viscous medium, the relaxation time relates to the rotational diffusion coefficient D as follows (*2*, *23*, *24*):

$$\tau = \frac{1}{2D} \tag{4}$$

To compare relaxation times, $\tau_{\eta,\mathrm{exp}}$, obtained in solvents with different viscosity, η_{exp}, the change in protein dynamics caused by a change in the solvent viscosity was taken into account. The relaxation times experimentally obtained were adjusted to the viscosity of water at 25 °C (η = 0.89 cP):

$$\tau_{\mathrm{exp}} = \tau_{\eta,\mathrm{exp}} \frac{\eta_{(\mathrm{H_2O},\,25\,^\circ\mathrm{C})}}{\eta_{\mathrm{exp}}} \tag{5}$$

Since a broad spectrum of motions is possible in long-chain molecules (*2*), it is worthwhile to note that anisotropy experiments report the average diffusion coefficient, or reciprocal average relaxation time, of motions that are comparable in time scale. Moreover, correlation times are averaged over conformational states (i.e., over substates) and probe orientations with respect to the principal axes of rotation.

RESULTS

Fluorescence anisotropy decay measurements were made for each globin in three conformational states: native, molten globule, and unfolded. More than 40 anisotropy decays were obtained under the different conditions. These include cosolvent cases intended to vary the rotational diffusion of the protein without disturbing the conformation. Typical examples of anisotropy kinetics observed in different conformational states of apoMb are shown in Figure 3. The fitted parameters (β_{fast}, ϕ_{fast}, β_{slow}, ϕ_{slow}), χ^2 values, initial anisotropy (r_o) and corresponding relaxation times (τ_{fast}, τ_{slow}) are summarized in Table 1.

Tryptophan nanosecond dynamics were well-described with a model of "two motions" for both one- and two-Trp proteins. The reduced χ^2 value, characterizing the goodness of the fit, was always less than 1.5, and the weighted residuals and the autocorrelation of the residuals were randomly distributed around zero, indicating an optimal fit. Importantly, the uncertainty of the model is strongly dependent on experimental conditions. For instance, the addition of sucrose to the protein solution (meant to vary only the rotational diffusion) increased the uncertainty of the relaxation parameters. Figure 4 shows the recovered $\chi^2 - \phi_{\mathrm{slow}}$ surfaces obtained for native protein when the sucrose concentration varied from 0 to 23 wt %. Clearly, at higher sucrose concentrations the $\chi^2 - \phi_{\mathrm{slow}}$ surface is more shallow; hence, the uncertainty of the relaxation time is greater. Indeed, the uncertainty may exceed 25−30% for a sucrose concentration of 23 wt %; i.e., at a level typically used for steady-state anisotropy experiments. This uncertainty is a consequence of the large ϕ/τ_{fl} ratio at higher viscosity, since the average lifetime of the Trp fluorescence, τ_{fl}, is about 2 $\sim$ 4 ns. More troubling, the relaxation time characterizing the overall rotation of the protein (see below) increases with protein concentration above 10 μM (Figure 5). It appears that native apoMb has a strong tendency toward aggregation even in highly dilute solutions. Both observations should be taken into account when dynamic parameters are recovered from the data of fluorescence experiments. In the present study, the protein concentration was always less than 6 μM.

Anisotropy in the Absence of Rotational Diffusion. An important characteristic obtained from the anisotropy profiles is the apparent "time zero" anisotropy r_o:

$$r_o = \beta_{\mathrm{fast}} + \beta_{\mathrm{slow}} \tag{6}$$

In general, the initial anisotropy is determined by the residue electronic structure. Yet, depending upon the freedom of the residue to rotate within the protein matrix, r_o may be reduced from expected values due to the presence of motion too rapid to be resolved experimentally. Subpicosecond studies on Trp-containing systems have shown that the theoretical r_o value of 0.4 (expected for collinear absorbance and emission dipoles) is not achieved (*25*). Early events in Trp fluorescence anisotropy kinetics and their relationship to protein structure are still under scrutiny.

Table 1 shows that in the native and molten globules the recovered initial anisotropy, r_o, has similar values of 0.23 ± 0.01 and 0.21 ± 0.01, respectively. These values are equivalent to the limiting anisotropy observed for tryptophanyl derivatives immobilized in poly(vinyl alcohol) films (*26*) or in propylene glycol (*27*), and to that observed for a wide range of peptides and native proteins in highly viscous media (*28*). In contrast, in the unfolded state, r_o values drop to 0.16 ± 0.01. This anisotropy reduction may be due to rapid motions that are missed (i.e., occur within the rise time of the apparatus), or may be a manifestation of electronic relaxation. Regarding Trp residue, nonrotational depolarization might arise from interactions of the ^1L_a and ^1L_b excited states; i.e., through vibronic coupling and vibrational relaxation (*25*). The experiments reveal, however, that a minor sucrose addition (9 wt %) leads to apparent r_o values of 0.21;

Table 1: Tryptophan Fluorescence Anisotropy Decay in Apomyoglobins[a]

protein source	β_{fast}	ϕ_{fast} (ns)	β_{slow}	ϕ_{slow} (ns)	χ^2	r_o	τ_{fast} ns	τ_{slow} ns	β_{fast}/r_o
native state (pH 6.5, 25 °C)									
sperm whale	0.05	0.5	0.19	7.0	1.36	0.24	1.5	21	0.21
sperm whale[b]	0.05	0.5	0.20	9.0	1.01	0.25	1.2	22	0.20
horse	0.04	0.5	0.17	7.0	1.11	0.21	1.5	21	0.19
tuna	0.06	0.5	0.17	7.9	1.23	0.23	1.5	24	0.26
W7F	0.05	0.2	0.16	8.9	1.29	0.21	0.6	27	0.24
W14F	0.06	0.3	0.17	10.3	1.29	0.23	0.9	31	0.26
molten globule state (pH 4.2, 25 °C)									
sperm whale	0.06	0.5	0.16	8.5	1.21	0.22	1.5	26	0.27
horse	0.06	0.6	0.16	9.0	1.33	0.22	1.8	27	0.27
tuna	0.06	0.5	0.14	10.0	1.23	0.20	1.5	30	0.30
W7F	0.03	0.4	0.16	9.3	1.3	0.19	1.2	28	0.19
W14F	0.06	0.3	0.17	10.5	1.29	0.23	0.9	31	0.26
unfolded state (pH 6.5, 25 °C, 8 M urea)[c]									
sperm whale	0.08	0.5	0.07	2.8	1.08	0.15	1.0	4.8	0.53
sperm whale[b]	0.12	0.5	0.09	4.7	1.46	0.21	0.9	5.6	0.57
horse	0.07	0.3	0.08	2.4	1.45	0.15	0.6	4.1	0.47
tuna	0.09	0.3	0.08	2.9	1.45	0.17	0.5	5.2	0.53
W7F	0.08	0.4	0.08	2.7	1.34	0.16	0.7	4.7	0.50
W14F	0.08	0.5	0.07	2.9	1.23	0.15	0.9	5.1	0.53

[a] The error in the values of recovered parameters is about 15% as been estimated through the analysis of χ^2-surfaces (see Materials and Methods) and the results of replication. [b] Solution with 9 wt % sucrose. [c] The relaxation times were adjusted to the viscosity of water at 25 °C ($\eta = 0.89$ cP).

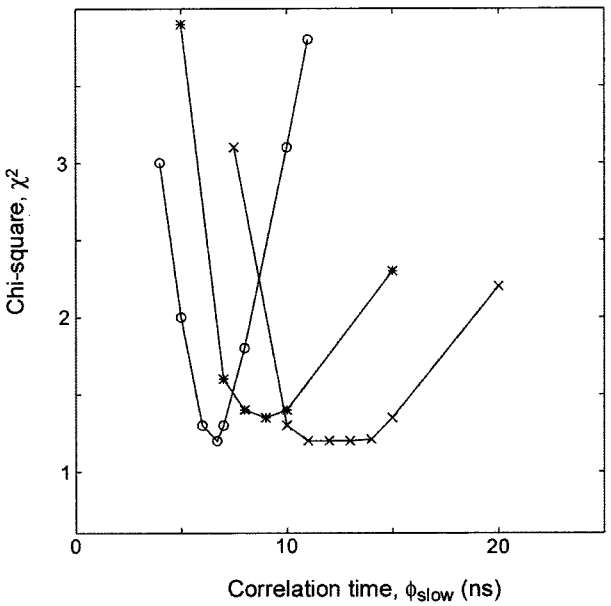

FIGURE 4: Example of ($\chi^2 - \phi$) surfaces recovered from the anisotropy decays of native apomyoglobin (sperm whale) in the presence of sucrose (left-to-right): 0, 9.3, and 23 wt %. The slow relaxation times (i.e., the overall protein rotation) are indicated by the minimum of the ($\chi^2 - \phi$) curves. The protein concentration was 4 μM in 10 mM sodium acetate, 10 mM sodium phosphate, and 30 mM NaCl at pH 6.5 and 25 °C.

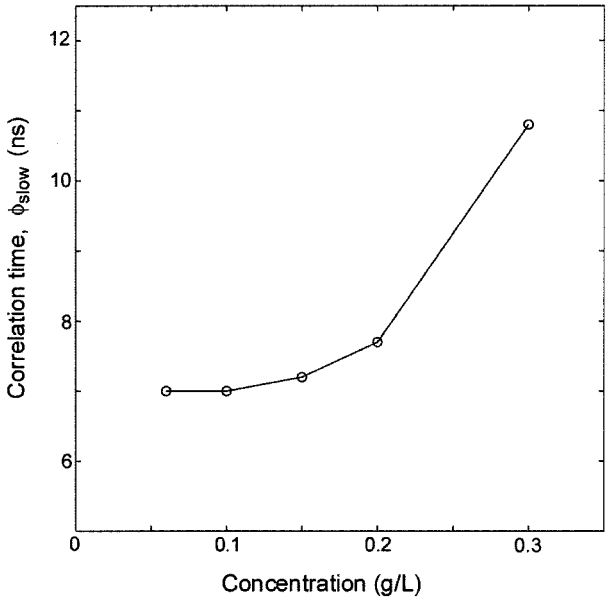

FIGURE 5: Effect of protein concentration c_{prot} on the time constant ϕ_{slow} of the slow relaxation process observed in the native state of horse apomyoglobin. The conditions were as described in Materials and Methods.

i.e., almost equal to that of native protein. No such effect of solvent viscosity on r_o is found for native molecules. Consequently, the smaller r_o observed in the unfolded globins is likely a result of Trp motion that is too rapid to be resolved by the present instrument with time resolution approaching 50 ps.

As to the observed reduction of the apparent $r_o \cong 0.22$ from the theoretical value of 0.4, potential explanations may include interactions of the ^1L_a and ^1L_b excited states (*25*, *29*), noncollinearity of absorption and emission dipoles (*23*, *30*, *31*), subpicosecond dynamics (*25*, *30*), and/or Trp↔Trp energy migration (*32*−*34*). The latter, however, cannot readily be applied to the globins. Indeed, the critical radius for Trp↔Trp energy migration in native globins is expected to be about 7 Å, which is very small in comparison with the Trp7−Trp14 separation of 12 Å reported for crystal structure. The predicted efficiency of Trp↔Trp energy migration should thus be only about 3%. More telling, similar r_o values are obtained for both one- and two-Trp globins (see Table 1). Another source of r_o reduction may be the simultaneous excitation of ^1L_a and ^1L_b states: at 295 nm, the ^1L_b excitation is expected to be small, but not necessarily zero. Figure 6 illustrates that both native and unfolded proteins yield similar Trp excitation spectra despite clear differences in Trp emission. Thus, the initial mixture of ^1L_a and ^1L_b is nearly the same for both conformational states. This, however, does not rule out subsequent nonrotational events that might

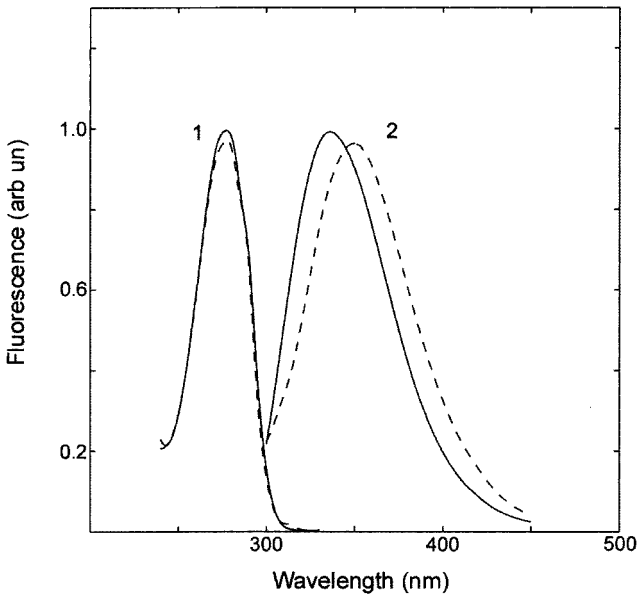

FIGURE 6: Steady-state fluorescence excitation (1) and emission (2) spectra of horse apomyoglobin in native (solid) and unfolded (dash) states. The excitation was set at 295 nm, and the emission was monitored at 350 nm. The conditions were as described in Materials and Methods.

reduce r_o. For these reasons, it is probably prudent to assume that the reduction in r_o observed in globins is a result of mixed excitation of ^1L_a and ^1L_b followed by rapid (2−4 ps) $^1L_b \rightarrow {}^1L_a$ relaxation, as suggested previously (*25*). Clearly, anisotropy measurements with subpicosecond time resolution and with the variation of both excitation and emission wavelengths are needed to understand how initial anisotropy of Trp is related to local protein structure. We have recently built a fluorometer to address these issues.

Nanosecond Dynamics of Tryptophan Residues. Two distinct kinds of Trp nanosecond mobility are evident in each conformational state of apoMb (Figure 3). The nature of the protein dynamics responsible for the decrease of Trp anisotropy in the different conformational states is different and needs to be addressed.

Compact Chain. The slow nanosecond relaxation process observed in native and molten globules is responsible for 80% of the decrease of anisotropy. This process might include the overall rotation of the protein with an average time τ_{whole}, and slow internal movements (rotation of subdomains, backbone, side chain, etc.) with an average time τ_{in} close to τ_{whole}:

$$\frac{1}{\tau_{exp}} = \frac{1}{\tau_{in}} + \frac{1}{\tau_{whole}} \qquad (7)$$

If one can measure τ_{exp} and independently evaluate the time of the overall rotation τ_{whole}, it might be possible to estimate the average time of slow internal rearrangements, τ_{in}, which the Trp residues report. For ellipsoidal particles with an axial ratio (p), the time of overall rotation can be calculated from the data of independent experiments as follows (*35*):

$$\tau_{whole} = \frac{3[\eta]\eta M}{\nu(p) RT} \qquad (8)$$

Here, M is the molecular weight of the protein, $[\eta]$ is the intrinsic viscosity of the protein solution, R is the gas constant, and T is the absolute temperature. The Simha factor $\nu(p)$ is a numerical coefficient depending on the molecular shape (*36*). For native apoMb molecules ($M = 17$ kD) in aqueous solution ($\eta = 0.89$ cP) at 25 °C with the experimental value of $[\eta] = 3.4 \pm 0.4$ cm^3/g (*37*, *38*), the time of overall rotation, τ_{whole}, was calculated to be 22 ± 3 ns, assuming the myoglobin molecule is a prolate ellipsoid with $\nu(1.76) = 2.8$ (*36*). Table 1 demonstrates that the slow times $\tau_{slow} = 24 \pm 3$ ns observed in native molecules are very close to the theoretical estimate for overall rotation. The prolate form of the body should, in fact, yield at least two rotational times (*39*, *40*). However, they are similar for a hydrated protein with this nearly spherical shape, and both exceed those of a sphere.

The slow motion observed in molten globules has the average time of 28 ± 2 ns. Meanwhile, the relaxation time calculated for overall rotation of the molten globule is 33 ns. This value corresponds to the 50% increase in the molecular volume directly observed at the "native molten globule" transition by viscosity measurements (*37*) and diffuse X-ray scattering experiments (*38*). The discrepancy between the theoretical and experimental values is only 15%; i.e., within experimental accuracy, they coincide. If one supposes, however, that in molten globules Trp residues are involved in another slow motion, then that internal rotation would need a time exceeding 120 ns. This estimate is obtained with eq 7, $\tau_{whole} = 33$ ns and τ_{exp} taken from Table 1.

The fast motion observed in compact states is responsible for 20% of the decrease of anisotropy and has an average relaxation time of 1.2 ± 0.2 ns. The mean amplitude of fast motion, characterized by the rotation angle θ, was calculated for different dynamic models (*23*, *41*, *42*) and gathered in Table 2. The analysis rules out the possibilities of both free rotation of the indole ring and a 180° ring flip observed for a few proteins by NMR (*43*). In fact, the fast Trp motion in globins appears to be restricted even in the unfolded states where θ reaches a maximum value of 39° (Table 2, part I). Yet, this motion cannot be simply ascribed to a free rotation of the emission dipole with a fixed valence angle (rotation on a cone). For instance, the angle between the ^1L_a dipole and the $C_\beta-C_\gamma$ bond is expected to be 90° (*30*) or 60° (*31*) for collinear and noncollinear absorbance and emission dipoles, respectively. These values are much larger than the 16°−28° calculated for the valence angle compatible with this model (Table 2, parts II and III). Perhaps the most feasible model is the free oscillation of the indole ring in a discrete potential hole of width θ (Table 2, parts IV and V). In this case, the mean amplitude of motion, θ, can be calculated as follows (*41*, *42*):

$$\frac{\beta_{fast}}{r_o} = 1 - \frac{\cos^2\theta(1+\cos\theta)^2}{4} \qquad (9)$$

Interestingly, a model for oscillation in azimuthal θ angle with a fixed valence angle (Table 2, part VI) gives similar results when applied to the rotation of a ^1L_a dipole around the $C_\beta-C_\gamma$ bond. Finally, the anisotropy experiments reveal that the average amplitude of fast Trp motions increases only slightly when the native globin ($\theta \cong 22°$) transfers to the molten globule state ($\theta \cong 25°$). Further, the amplitudes

Table 2: Mean Amplitude of Tryprophan Fast Motions in Apomyoglobin

model	$\left[1-\frac{\beta_{fast}}{r_o}\right]^a =$	θ^b N	MG	U
I. rotation on θ angle (*23*)	$\frac{3(\cos^2\theta)-1}{2}$	21	25	36
II. free rotation with fixed valence θ angle (*23, 41*)	$\left[\frac{3(\cos^2\theta)-1}{2}\right]^2$	16	18	28
III. axially symmetric oscillation about fixed axis (*41*)		16	18	28
IV. free diffusion within in the cone of semi angle θ (42)[c]	$\left[\frac{\cos\theta\,(1+\cos\theta)}{2}\right]^2$	22	25	39
V. oscillation in discrete potential hole of θ_m width[c] (*41*)		22	25	39
VI. oscillation in azimuthal θ angle with fixed valence α angle[d] (*41*)	$1-\frac{3\sin^4\alpha(\sin 2\theta)^2}{4}-\frac{3\sin^2 2\alpha(\sin\theta)^2}{4}$	15	17	28
		20	21	34

[a] Average values been taken from Table 1. [b] Calculated for native (N), molten globule (MG), and unfolded (U) states. [c] The model implies the existence of a square-well potential, which restricts rotation. [d] Valence (α) angle between ^1L_a emission dipole and $C_\beta-C_\gamma$ bond was taken as 90° (first row) and 60° (second row).

Table 3: Slow Nanosecond Relaxation Process in Unfolded Polypeptide Chain

protein	molecular weight	conditions[a]	ϕ_{exp} (ns)	τ_{red}[b] (ns)	refs
melittin	2846	D_2O, pH 4		3.6	(*49*)
glucagon (peptide 2)	3482	pH 7	1.51	4.5	(*47*)
adrenocorticotropic hormone	4811	pH 7	2.06	6.2	(*47*)
G-actin	4900	8 M urea		~4	(*32*)
monellin	5835	5 M GuHCl	1.76	3.8	(*3*)
protein G[c]	6500	6 M GuHCl	2.4	4.6	
Glu-Leu-Trp[d]	6500	0.2 M NaCl, pH 7		3.6	(*48*)
Glu-Trp[e]	7000	0.2 M NaCl, pH 7		3.8	(*48*)
myelin basic protein	14818	35 °C	1.7	6.2	(*3*)
Glu-Trp[e]	15000	0.2 M NaCl, pH 7		3.8	(*48*)
apomyoglobins[c]	16951	8 M urea	2.7	4.7	
glucagon	18212	19 °C	1.67	5.0	(*45*)
tumor necrosis factor-α	25644	4.2 M GuHCl	1.5	3.5	(*46*)
human serum albumin	69000	44 °C, 6 M GuHCl	1.5	4.1	(*3*)
elongation factor G	81000	8.5 M urea		4.1	(*48*)

[a] Measurements were carried out at 20 °C unless stated. [b] The relaxation times were adjusted to the viscosity of water at 25 °C ($\eta = 0.89$ cP). [c] Present investigation. [d] Statistical copolymer of L-glutamic acid (82.5%), L-leucine (17%), and L-tryptophan (0.05%). [e] Statistical copolymer of L-glutamic acid (99.5%) and L-tryptophan (0.5%).

reported by the one-Trp proteins are very comparable to those of the two-Trp samples.

Unfolded Chain. The rotational freedom of the Trp residues substantially increases upon unfolding. Therefore, the system loses anisotropy much faster in the unfolded state than in the native or molten globule states (Figure 3). Even in the unfolded molecules, however, the anisotropy continues to resolve two distinct motions with relaxation times of 0.8 ± 0.2 ns and 4.9 ± 0.4 ns. Both relaxation processes contribute equally; i.e., each is responsible for 50% of the anisotropy decrease.

In a manner analogous to the previous analysis, a "slow" motion observed in the unfolded globins can be considered as a superposition of an overall rotation and some average internal movement. For unfolded apoMb molecules in aqueous solution at 25 °C with the experimental value of $[\eta] = 20.9$ cm^3/g (*37*, *44*) the expected time of overall rotation is about 250 ns.[2] On the time scale of Trp fluorescence (~4 ns), such slow rotations are imperceptible. Consequently, the average relaxation time τ_{exp} practically coincides with the average time τ_{in} of intramolecular motions (eq 7), i.e., backbone and side-chain mobility. To understand which relaxation process is dominant, one may refer to data obtained for other Trp-containing macromolecules. Table 3 demonstrates that a relaxation process with a time of 4~6 ns is quite typical for unfolded proteins (*3*, *32*, *45*, *46*), adrenocorticotropic hormones (*47*), and synthetic polypeptides (*48*, *49*). Note that this "slow" motion seems nearly independent of amino acid sequence. Moreover, this time (4~6 ns) is considerably smaller than that of backbone relaxation (30~40 ns), which has been measured independently for labeled polypeptides by the method of polarized luminescence (*2*, *48*). Furthermore, a recent NMR and fluorescence study on synthetic polypeptides has revealed similar nanosecond relaxation for the Trp side chain in random coil and helical conformations (*49*). Obviously, the backbone mobility is markedly different in these conformational states (*2*). This suggests that the "slow" relaxation process reported by anisotropy decay of unfolded apoMb chains arises from local mobility of the side chain of the Trp residue; i.e., from rotation of the indole ring about the $C_\alpha-C_\beta$ and $C_\beta-C_\gamma$ bonds, jumping from one rotational isomeric hole to another.

The rate of the faster movement observed in the globins shows almost no sensitivity to the structure of the protein

[2] For coillike macromolecules the $3/\nu(p)$ coefficient in eq 8 has a value of 2 (*35*).

molecule. The relaxation times vary only slightly upon protein unfolding, going from 1.2 ns (native) to 0.8 ns (unfolded). The amplitude, however, increases from 25° (native) to 39° (unfolded). It is reasonable to assign this most rapid Trp motion to the oscillations (torsional vibration) of the indole rings within their allowed potential holes. At this juncture, some speculation about the recovered τ values can be made. Nanosecond relaxation processes in macromolecules with internal rotation or torsional vibrations immersed in a viscous solvent with viscosity $\eta \sim 1$ cP are well-described in a vast majority of cases by the following equation (*2*):

$$\frac{1}{\tau_j} = a_j\left(\frac{T}{\eta}\right)\exp\left[-\frac{U_j}{kT}\right] \qquad (10)$$

where a_j is a rotation rate depending only on the temperature T and solvent viscosity η, and U_j is the energetic barrier to internal motion in the backbone or side chain. Comparison between relaxation times of rotational isomerization ($\sim$5 ns) with that of torsional vibrations (0.8 ns) thus allows an estimation of the relative potential barrier expected for the rotational isomerization in globins. The calculations show that in unfolded protein, this barrier is only about 1 kcal/mol; i.e., the Trp rotamers are expected to be easily interconvertible with the expenditure of a relatively small amount of energy. For uncorrelated rotations about the $C_\alpha-C_\beta$ and $C_\beta-C_\gamma$ bonds, one may thus infer that the jump from one isomeric hole to another is largely due to the rotation about the $C_\beta-C_\gamma$ bond. Clearly, the barrier for rotation around $C_\alpha-C_\beta$ bond should not be less than 3 kcal/mol, the barrier for ethane (*48*, *50*). For the latter, the fast relaxation time is expected to be about 30 ps (see eq 10). This is considerably faster than the measured fast relaxation in globins ($\sim$1 ns) or even the solvent limited rotation rate for free tryptophan (ca. 100 ps). Otherwise, it could be more complex, correlated motion about both bonds.

Time-resolved Fluorescence Intensity Decay. The fluorescence intensity decays were measured across the emission spectrum for all proteins studied. The detailed analysis of the DAS will be reported elsewhere; here, we discuss only the most general features. Two fluorescence lifetimes were needed to describe adequately the fluorescence intensity kinetic in both the globins with one- or two-Trp residues. Figure 7 shows the DAS for sperm whale apoMb recorded in different conformational states. In the native state, the spectrum associated with the short lifetime (1.3 ns) is the major contributor ($\sim$70%), with an emission maximum located at 330 nm. The spectrum associated with the long lifetime (4.1 ns) provides a minor contribution ($\sim$30%) and has an emission maximum at 335 nm. These data correspond well to those reported previously (*34*, *51*). In the molten globules, the spectrum of a new longer component (5.8 ns) is dominant, and the short lifetime component (1.8 ns) represents only 35% of the total fluorescence. Importantly, the spectra are clearly separated by 5 nm in both compact states (Figure 7, inset). In contrast, for unfolded molecules, spectra associated with the long (4.7 ns) and short (1.7 ns) decay components have similar spectral properties in terms of maximum position at 350 nm and spectral shape (Figure 7, inset). The progression of DAS shifts toward indistinguishability has been seen so far only in yeast arginase during stepwise unfolding after structural metal removal (*52*). In general, a shift between DAS components testifies to the existence of at least two fluorescence species located in distinct environments. In the globins, the observed two-component DAS might either be correlated with the individual Trp residues (when both are present), or with rotamers of the Trp side chain, or with the structural heterogeneity and rigidity in the vicinity Trp residues. In the unfolded state, however, DAS report a homogeneous environment for both Trp residues as well as their possible substates. The molecular mechanism of fast averaging in the unfolded polypeptide chain appears to be an internal motion with relaxation time of 5 ns. In other words, the interconversion from one possible environment to another occurs during the Trp fluorescence lifetime of $\sim$4 ns.

DISCUSSION

Time-resolved fluorescence studies with Trp residues as intrinsic fluorophores were performed with one- and two-Trp globins from different sources. The simple "two-time approximation" employed to describe the complex nanosecond dynamics of these globins was well-suited to different conformational states (native, molten globule, and unfolded). The most significant difference among the proteins investigated is that sperm whale and horse globins contain two Trp residues located at positions 7 and 14, whereas the others contain a single Trp residue at either position 14 (sperm whale W7F, tuna) or 7 (sperm whale W14F). The different fluorescent properties of the Trp residues in apoMb have been discussed intensively over the past decade (*8*, *12*, *13*). It has been suggested (*13*) that, in the native state, the fluorescence quantum yield of Trp14 is 2-fold higher than that of Trp7. Meanwhile, in the molten globule state, the situation reverses. These data (*13*) led to the conclusion that heterogeneity of the Trp fluorescence are complex, and that this must to be taken into account for anisotropy analysis. In the present experiments, however, almost identical anisotropy decays were found for various apomyoglobins and their variants. Importantly, the relaxation parameters of globins with two Trp residues are very comparable to those of globins with only a single Trp residue. Unexpectedly, heterogeneity of the Trp fluorescence has only small effects on the relaxation parameters recovered from the anisotropy decay profiles.

All globins show very similar changes in molecular dynamics throughout protein (un)folding. A very rapid relaxation component, $\tau < 1$ ns, can be ascribed to subnanosecond oscillations (torsional vibrations) of the indole ring inside the rotameric hole. This process causes a very fast depolarization and, most importantly, it is not appreciably influenced by the protein structure. Similar results have been reported recently for cytochrome b_5 (*53*). Conversely, a longer relaxation process is very sensitive to the formation of the compact conformational state. In the native and molten globule states, the nanosecond relaxation spectrum is dominated by the contribution (80%) of an overall rotation of the protein molecule. A smaller contribution (20%) comes from torsional vibrations of the indole groups within their rotational isomers. In the unfolded state, the nanosecond relaxation spectrum is composed of equal contributions from the torsional vibrations and isomeric rotation of the indole groups, likely about $C_\beta-C_\gamma$ bonds.

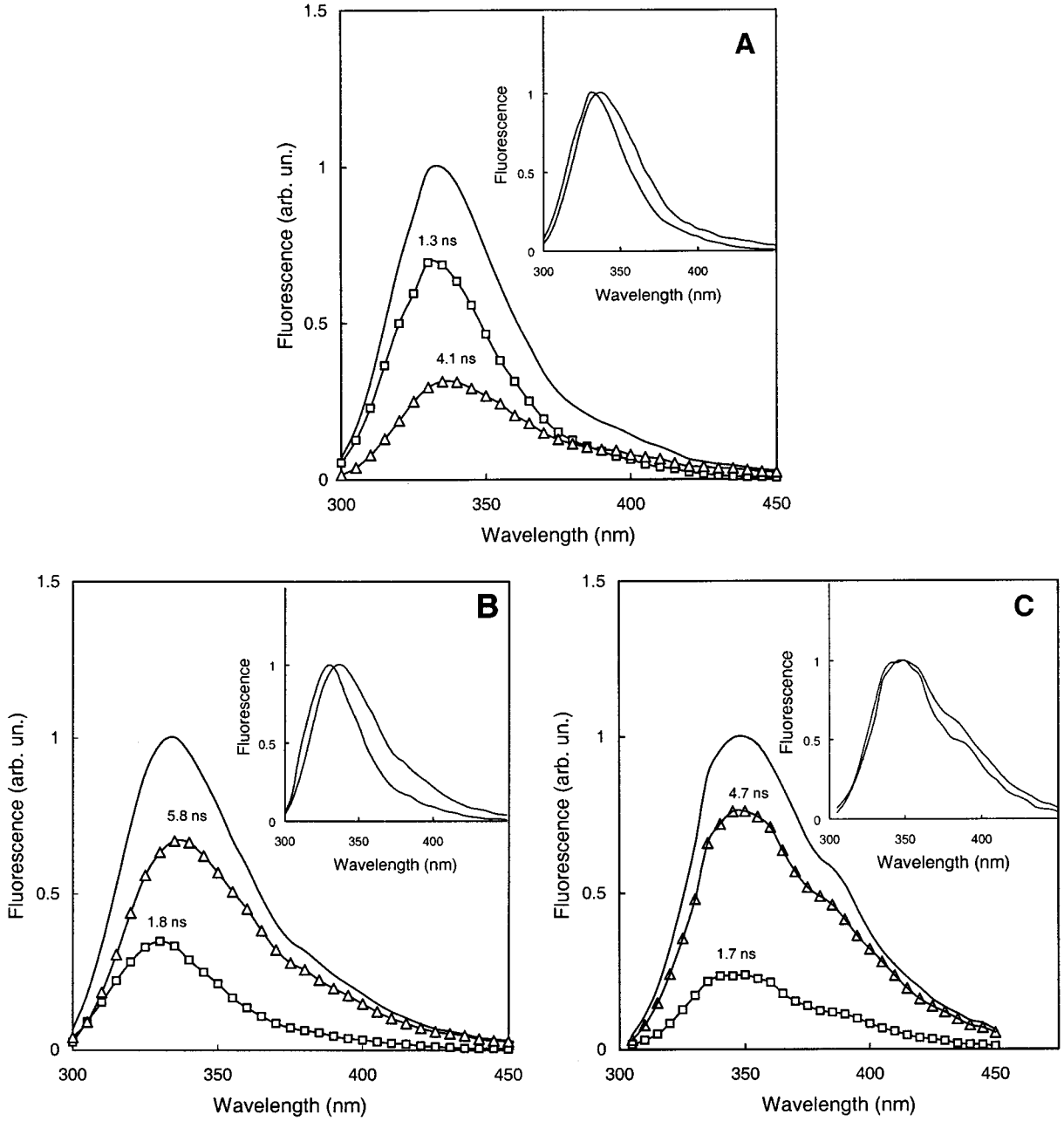

FIGURE 7: Resolution of the total fluorescence spectrum of sperm whale apomyoglobin in native (A), molten globule (B), and unfolded (C) states into decay-associated spectra. Each decay component with long (△) and short (□) lifetime (indicated on the top of spectrum) are shown. Insert shows the normalized spectral distribution of each component. The experimental conditions were described in Materials and Methods.

Of particular interest is the evolution of the nanosecond dynamics during protein folding. As mentioned above, the Trp residues in globins are located in the A-helix fragment of the protein chain (Figure 1). Multidimensional NMR spectroscopy has revealed that the native A, G, H-helices of apoMb become relatively stable at an early stage of protein folding and are relatively stable in the equilibrium molten globule state (*54*). The structure of the AGH subdomain in the molten globule states, however, is still unclear. From the anisotropy experiments, we conclude that the "unfolded−molten globule" transition leads to considerable inhibition of the internal rotation of the Trp side chain. Specifically, the time of internal rotation changes from 5 ns (unfolded) to >120 ns (molten globule), i.e., increases more than 20-fold. Experiments with helical polypeptides, however, reveal considerably smaller changes in Trp side chain mobility upon the formation of helical structure (*48*, *49*). For instance, in statistical copolymers of glutamic acid or lysine with L-tryptophan, the time of rotational isomerism (4−5 ns) increases in the "coil−helix" transition by only 1 ns. The statistical introduction of 17% of hydrophobic leucine groups to copolymers leads to an increase of relaxation time at the "coil−helix" transition by only 5 ns (*48*). At this juncture, the relaxation behavior observed in apoMb at the "unfolded−molten globule" transition most likely can be explained by the aggregation of the A, G, and H helical regions in the molten globule state, and by involvement of the Trp residues in the formation of the helical interfaces.

Further, the Trp nanosecond dynamics change very little over the "molten globule−native" transition. The slow relaxation process corresponds to the overall rotation of the protein molecule, with time constants of 28 ± 3 ns and 22

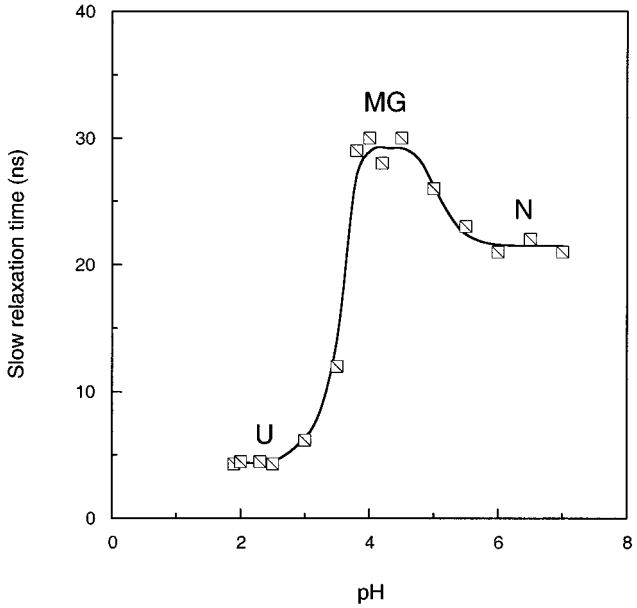

FIGURE 8: The unfolding of horse apomyoglobin followed by the slow relaxation time recovered from the fluorescence anisotropy kinetics of tryptophan residues.

± 1 ns for the molten globule and native states, respectively. The amplitude and rate of rapid torsional vibrations of the Trp side chains are very similar in both states. On the other hand, the amplitude of fast motion observed in polymer chains is seen as a sensitive measure of tight packing in compact macromolecular structures (*2*). Thus, the similarities we observe for fast motions in both compact states lead us to conclude that in the molten globule state the Trp residues of the A-helix are involved in native-like tertiary interactions. This conclusion is in good agreement with results of molecular dynamics simulations characterizing the structural fluctuations of apoMb in native and molten globule states (*55*). These experiments show that, in both states, the GH segment interacts with the conformationally non-labile helix A to form a relatively rigid AGH subdomain. The highly restricted local rotation of the Trp residues of the A helix in the molten globule state and the similarity of the Trp relaxation spectra in native and molten globule states corroborate the suggestion that the A-, G-, and H-helices in the molten globule state of apoMb constitute a native-like subdomain (*56*). Hence, the conformation changes that distinguish the molten globule and native states result from either subtle, slow (>120 ns) rearrangements or those peripheral in location to the Trp residues.

In addition, another important aspect of the conformational rearrangements observed in apoMb needs to be addressed. Recently, it has been suggested that the molten globule state of apoMb (induced by urea or pH) is split into two different intermediates (*57*). Figure 8 illustrates the changes in slow relaxation time for the (un)folding of apoMb induced by pH. Three conformation states (native, molten globule, and unfolded) are clearly visible. Importantly, that in the range of pH 3.6−4.3 (molten globule state), anisotropy experiments report similar nanosecond dynamics related to the overall rotation of the protein. It appears that small (∼5%) fluorescence changes observed in ref *57* most probably reflect the variety of local conformations within the molten globule state, i.e., the variety of molten globule substates.

ACKNOWLEDGMENT

To our great sorrow, Oleg B. Ptitsyn passed away on March 22, 1999. He initiated this work, provided proteins, and participated in all stages of data analysis. We will remember him as a great scientist, teacher, and friend. We express our sincere appreciation to Robert Jernigan for enormous support of this research and to Stewart R. Durell for critically reading the manuscript. We thank Valentina Bychkova for sample preparations and Denise Porter for assistance in anisotropy measurements.

REFERENCES

1. Ptitsyn, O. B. (1995) *Adv. Protein Chem. 47*, 83−229.
2. Anufrieva, E. V., and Gotlib, Yu. Ya. (1981) *Adv. Polym. Sci. 40*, 1−68.
3. Lakowicz, J. R. (1983) *Principles of Fluorescence Spectroscopy*, pp 342−381, Plenum Press, New York/London.
4. Kuznetsova, I. M., and Turoverov, K. K. (1983) *Mol. Biol. (Moscow) 17*(*4*), 741−754.
5. Haouz, A., Glandieres, J. M., Zentz, C., Pin, S., Ramstein, J., Tauc, P., Brochon, J. C., and Alpert, B. (1998) *Biochemistry 37*(9), 3013−3019.
6. Knutson, J. R., Davenport, L., and Brand L. (1986) *Biochemistry 25*(*7*), 1805−1810.
7. Bismuto E., Gratton, E., Sirangelo, I., and Irace, G. (1993) *Eur. J. Biochem. 218*, 213-219.
8. Rischel, C., Thyberg, P., Rigler, R., and Poulsen, F. M. (1996) *J. Mol. Biol. 257*, 877−885.
9. Lakowicz, J. R., Gratton, E., Cherek, H., Maliwal, B. P., and Laczko, G. (1984) *J. Biol. Chem. 259*, 10967−10972.
10. Bucci, E., and Steiner, R. F. (1988) *Biophys. Chem. 30*, 199−124.
11. Barrick, D., and Baldwin, R. L. (1993) *Biochemistry 32*, 3790−3796.
12. Irace, G., Balestrieri, C, Parlato, G., Servillo, L., and Colonna G. (1981) *Biochemistry 20*, 792−799.
13. Postnikova, G. V., Komarov, Yu. E., Yumakova, E. M. (1991) *Eur. J. Biochem. 198*, 223−232.
14. Teale, F. W. J. (1959) *Biochim. Biophys. Acta 35*, 543.
15. Laemmli, U. K. (1970) *Nature 227*, 680−685.
16. Gill, S. C., and von Hippel, P. H. (1989) *Anal. Biochem. 182*, 319−326.
17. Shen, F., Triezenberg, S. J., Hensley, P., Porter, D., and Knutson, J. R. (1996) *J. Biol. Chem. 271*, 4819−4826 (and reference therein).
18. Knutson, J. R., Beechem, J. M. and Brand, L. (1983) *Chem. Phys. Lett. 102*, 501−507.
19. Knutson, J. R., Walbridge, D. G., and Brand, L. (1982) *Biochemistry 21*, 4671−4679.
20. Beechem, J. M., Gratton, E., Ameloot, M., Knutson, J. R., and Brand, L. (1991) In *Topics in Fluorescence Spectroscopy* (Lakowicz, J. R., Ed) Vol 2, pp 241−305, Plenum Press, New York (references therein).
21. Johnson, M. L., and Faunt, L. M. (1992) *Methods in Enzymology* (Brand, L., Johnson, M. L., Eds) Vol 210, pp 1−37.
22. Tcherkasskaya, O., Spiro, J. G., Ni, Sh., and Winnik, M. A. (1996) *J. Phys. Chem. 100*, 7114−7121.
23. Steiner, R. F. (1991) In *Topics in Fluorescence Spectroscopy* (Lakowicz, J. R., Ed) Vol 2, pp 1−52, Plenum Press, New York.
24. Creighton, T. E. (1993) *Proteins: Structure and Molecule Properties*; pp 268, W. H. Freeman Company, New York.
25. Ruggiero, A. J., Todd, D. C., and Fleming, G. R. (1990) *J. Am. Chem. Soc. 112*, 1003−1014.
26. Konev, S. V. (1967) *Fluorescence and Phosphorescence of Proteins and Nucleic Acids*, pp 30−33, Plenum Press, New York.
27. Valeur, B., and Weber, G. (1979) *Photochem. Photobiol. 25*, 441−444.
28. Lakowicz, J. R., Maliwal, B. P., Cherek, H., and Balter, A. (1983) *Biochemistry 22*, 1741−1752.

29. Callis, P. R. (1997) *Methods Enzymol. 278*, 113−150.
30. Ichiye, T., and Karplus, M. (1983) *Biochemistry 22*, 2884−2893.
31. Yamamoto, Y., and Tanaka, J. (1972) *Bull. Chem. Soc. Jpn. 45*, 1362−1366.
32. Turoverov, K. K., Biktashev, A. G., Khaitlina, S. Yu., and Kuznetsova, I. M., (1999) *Biochemistry 38*, 6261−6269 (and references therein).
33. Bialik, C. N., Wolf, B., Rachofsky, E. L., Ross, J. B. A., and Laws, W. R. (1998) *Biophys. J. 75*, 2564−2573.
34. Eftink, M. R., Wasylewsky, Z., and Chiron, C. A. (1987) *Biochemystry 26*, 8338−8346.
35. Ptitsyn, O. B., and Eizner, Y. E. (1959) *Z. Tekh. Fix. 23*, 1112−1134.
36. Cantor, C. R., and Schimmel, P. R. (1980) *Biophysical Chemistry*, pp 561−665, W. H. Freeman Company, New York.
37. Griko, Yu. V., Privalov, P. L., Venyaminov, S. Yu., and Kutyshenko, V. P. (1988) *J. Mol. Biol. 202*, 127−138.
38. Kataoka, M., Nishii, I., Fejisawa, T., Ueki, T., Tokunaga, F., and Goto, Y. (1995) *J. Mol. Biol. 249*, 215−228.
39. Tao, T. (1969) *Biopolymers 8*, 609−632.
40. Beechem, J. M., Knutson, J. R., and Brand, L. (1986c) *Biochem. Soc. Trans. 14*, 832−835.
41. Anufrieva, E. V., Gotlib, Yu. Ya., Krakovyak, M. G., and Pautov, B. D. (1976) *Vysokomol. Soedin. A 18*, 2740−2746.
42. Lipari, G., and Szabo, A. (1980) *Biophys. J. 30*, 489−506.
43. Wüthrich, K. (1995) *NMR in Structural Biology*, pp 576−583, World Scientific Publishing Co. Pte. Ltd., Singapore.
44. Tanford, C., Kawahara, K., and Lapanje, S. (1967) *J. Am. Chem. Soc. 89*, 729−736.
45. Tran, C. D., Beddard, G. S., and Osborne, A. D. (1982) *Biochim. Biophys. Acta 709*, 256−264.
46. Kim, Y.-R., Hahn, J. S., Hong, H., Jeong, W., Song, N. M., Shin, H. L., and Kim, D. (1999) *Biochim. Biophys. Acta 1429*, 486−495.
47. Chen, L. X.-Q., Petrich, J. W., Fleming, G. R., and Perico, A. (1987) *Chem. Phys. Lett. 139*, 55−61.
48. Semisotnov, G. V., Zikherman, K. Kh., Kasatkin, S. B., Ptitsyn, O. B., and Anufrieva E. V. (1981) *Biopolymers 20*, 2287−2309 (and reference therein).
49. Kemple, M. D., Buckley, P., Yaun, P., and Prendergast, F. (1997) *Biochemistry 36*, 1678−1688.
50. Orville-Thomas, W. J. (1974) In *Internal Rotation in Molecules*. (Orville-Thomas, W. J., Ed), pp 1−19, John Wiley & Son, London.
51. Janes, S. M., Holtom, G., Ascenzi, P., Brunori, M., and Hochstrasser, R. M. (1987) *Biophys. J. 51*, 653−660.
52. Green, S. M., Knutson, J. R., and Hensley, P. (1990) *Biochemistry 29*, 9159−9168.
53. Storch, E. M., Grinstead, J. S., Campbell, A. P., Dagget, V., and Atkins, W. M (1999) *Biochemistry 38*, 5065−5075.
54. Eliezer, D., Yao, J., Dyson, H. J., and Wright, P. E. (1998) *Nat. Struct. Biol. 5*(*2*), 148−155.
55. Brooks, C. L. (1992) *J. Mol. Biol. 20*, 375−380.
56. Hughson, F., Wright, P., and Baldwin, R. (1990) *Science 249*, 1544−1548.
57. Jamin, M. and Baldwin. R. L. (1998) *J. Mol. Biol. 276*, 491−504.

BI992117+